PART II.1

IDENTIFICATION METHODS FOR HYPERFRAGMENTS*)

R.G. Ammar,

Physics Department, Northwestern University,
Evanston, Ill., USA.

I. INTRODUCTION

Information relevant to the identification of hyperfragments may be classified into three general categories accordingly as it is derived from the configuration at production, from that at decay, or from information regarding charge and mass supplied by direct measurements on the tracks themselves. In order to obtain a unique identification for an event it is obviously necessary to impose a sufficient number of constraints to rule out all but one hypothesis regarding its interpretation. Thus, although the three categories will be discussed separately it should be borne in mind that information of more than one type is often used in the analysis of a single event.

For purposes of orientation as regards the energy released at production and decay, some typical reactions are given in Table 1, together with their corresponding energies. These values will, of course, be modulated by effects arising from the binding of the particles involved in any particular reaction, an appreciable effect for the π^- decays. Nevertheless, the relative magnitudes of these energies give some indication as to the type of problems which one might expect to encounter in the different processes.

In the ensuing discussion of the various methods of identification I shall confine my remarks primarily to hyperfragments produced in nuclear emulsion, as other talks have been scheduled which will deal with work performed in bubble chambers.

---

*) Research supported by the National Science Foundation.

Table 1

Some characteristic reaction energies in Λ production and decay

Reaction	Energy release (MeV)
$K^- + 2p \rightarrow \Lambda + p$	316.7
$K^- + n \rightarrow \Lambda + \pi^-$	178.4
$\Lambda + p \rightarrow n + p$	175.9
$\Lambda \rightarrow p + \pi^-$	37.6

II. PRODUCTION CONFIGURATION

Kinematic considerations at production have already been used by many authors[1-7] as an auxiliary method in the identification of hyperfragments produced by K^- and Σ^- capture in emulsion. In addition, systematic investigations have been made relating to this production process, establishing the fact that hypernuclei with charge $Z \geq 3$ are primarily from the light elements (C, N, O) of the emulsion[8-12].

The power of this method tends to increase with the mass number A of the hyperfragment produced (for $A \leq 16$), since the permissible production reactions become simpler. It is therefore ideally suited to augment the analysis of the π^- decays of hypernuclei with $5 < A \leq 16$ where the information at decay is usually less complete than for those with $A \leq 5$ (see Section III). In addition, a particularly good illustration of the usefulness of this approach may be found in the problem of identifying non-mesic decays where the large energy release and the emission of neutrons makes a decay analysis by itself

rather unreliable. At present a systematic investigation of such decays of hypernuclei with $Z \geq 3$ is under way in our laboratory using production kinematics as a tool[13,14]. To facilitate the analysis, only those hyperfragments produced in association with a charged π from K^- captures are considered. Thus events produced with a π^0 or with no pion and which are somewhat more difficult to analyse, are excluded from the sample. The production process under consideration is, however, not necessarily confined to the second of the reactions in Table 1 since an appreciable fraction ($\gtrsim 7\%$) of the charged pions are π^+ and cannot be produced in association with a Λ via K^- capture on a single nucleon.

Figure 1 shows a photomicrograph of an event analysed in this manner. The primary π^- is brought to rest after ~ 2.8 cm and the production reaction is most likely given by

$$K^- + C^{12} \rightarrow {}_{\Lambda}Be^9 + H^1 + H^1 + n + \pi^-$$

although one cannot rigorously rule out the possibility that some other isotope of ${}_{\Lambda}Be$ is produced with more than one neutron. The deday, however, is ambiguous and although consistent with that of ${}_{\Lambda}Be^9$, is also consistent with many other interpretations.

The dimensions of the stack ($\sim$ 10 cm $\times$ 15 cm $\times$ 10 cm) used in this work was designed primarily to stop pions from the decay reaction. Thus, because of the much larger energy release at production, $\sim 60\%$ of the pions could not be followed to rest in the stack. In such cases, ionization measurements on the pion can still yield much useful information in the analysis of the event.

III. DECAY CONFIGURATION

The analysis of the π^--mesic decays of hypernuclei with $A \leq 5$ is fairly straightforward and has been discussed, for example, in Refs. 15 and 16. For such events, the decay prongs are comparatively

well defined and the concept of coplanarity and colinearity of tracks is meaningful, in contrast to the case for A > 5, so that the application of momentum conservation is frequently sufficient to yield a unique interpretation. Even so, for short recoils, misidentification of events can take place as may be seen with reference to Fig. 2 showing a recoil range versus momentum, taken from Ref. 16. Such misidentification may introduce systematic errors in the measured binding[17] since, for example, ${}_{\Lambda}He^{5}$ has a higher binding than ${}_{\Lambda}He^{4}$ and if misinterpreted as the latter, will tend to increase the measured binding for ${}_{\Lambda}He^{4}$.

For the heavier hypernuclei, the problem of identification is somewhat more difficult. A large number of the decays (e.g. ~ 50% of the events presented in Ref. 5) consist of only a π^- and a stub, usually too short to permit a precise measurement of its range and direction. Thus the recoil can not usually be identified from momentum balance. Information bearing on the recoil identity can be obtained by observing whether it undergoes β decay with a half-life short compared with the sensitive time of the detector. Figure 3 shows an event interpreted as ${}_{\Lambda}B^{11} \rightarrow \pi^- + C^{11}$ in which a β is associated with the recoil. In exceptional cases the identity of the recoil may be inferred from its decay (e.g. a "hammer track" configuration). Such an event, interpreted as ${}_{\Lambda}Li^{9} \rightarrow \pi^- + H^{1} + Li^{8}$, is shown in Fig. 4. For this event the interpretation of the "hammer track" as B^8 can be ruled out by detailed considerations[5]. Examples of both types of events were already presented in Ref. 5.

Information regarding the $(\pi^- - r)$ decay mode of hypernuclei with $6 \leq A \leq 16$, already presented in Refs. 4 and 5, is summarized in Fig. 5. Not all the species shown in this figure are known to exist. Their decays are separated into two groups depending on whether or not a β is expected to be seen from the recoil. The $(\pi^- - r)$ mode is, however, not the only one which can give rise to this type of configuration. Table 2 presents a list of values for Q_o (the energy release assuming zero binding for the Λ), as well as the expected energy release

Table 2

Characteristics of $(\pi^- - n - r)$ decays
for hypernuclei with mass number ≤ 16

Hypernuclide	Q_o (MeV)	$\sim Q$ (MeV)	Recoil: Identity	Recoil: Decay	Recoil: Half-life (sec)
${}_\Lambda H^4$	36.81	34.7	He^3		Stable
${}_\Lambda He^7$	40.33	36.5	Li^6		Stable
${}_\Lambda Li^8$	35.93	29.4	Be^7	K capture	4.6×10^6
${}_\Lambda Li^9$	52.80	44.8	Be^8	$He^4 + He^4$	$< 2 \times 10^{-14}$
$({}_\Lambda Li^{10})$	50.89	41.9	Be^9		Stable
${}_\Lambda Be^9$	18.82	12.3	B^8	Hammer	0.8
$({}_\Lambda Be^{11})$	37.35	27.9	B^{10}		Stable
$({}_\Lambda Be^{12})$	48.27	37.8	B^{11}		Stable
${}_\Lambda B^{11}$	33.02	23.1	C^{10}	β^+	19.1
${}_\Lambda B^{12}$	34.82	24.4	C^{11}	β^+	1.2×10^3
$({}_\Lambda B^{13})$	50.17	38.2	C^{12}		Stable
$({}_\Lambda B^{14})$	50.23	36.7	C^{13}		Stable
${}_\Lambda C^{13}$	19.34	8.5	N^{12}	β^+	0.012
${}_\Lambda C^{14}$	34.57	21.4	N^{13}	β^+	606
$({}_\Lambda C^{15})$	36.95	22.5	N^{14}		Stable
$({}_\Lambda C^{16})$	46.57	31.1	N^{15}		Stable
$({}_\Lambda N^{15})$	31.65	17.2	O^{14}	β^+	76.5
$({}_\Lambda N^{16})$	34.04	18.5	O^{15}	β^+	124

The species in parenthesis have not been uniquely identified. In calculating Q, B_Λ has been inferred from the trend of the B_Λ versus A curve.

5683/NP/kw

Q, for various $(\pi^- - n - r)$ decay modes. For the more massive species, these decays will present the same appearance as the $(\pi^- - r)$ events. In addition, so can more complex decay modes involving three charged particles. Some of these are shown in Table 3 which lists only those for which both heavy particles in the final state have $Z \geq 3$.

Table 3

Complex decays of hypernuclei with mass number ≤ 16 which may simulate the $(\pi^- - r)$ mode

Decay	Q_o (MeV)	$\sim Q$ (MeV)
${}_{\Lambda}B^{12} \rightarrow \pi^- + Li^6 + Li^6$	25.35	15.0
$({}_{\Lambda}B^{13} \rightarrow \pi^- + Li^6 + Li^7)$	29.24	17.2
$({}_{\Lambda}B^{14} \rightarrow \pi^- + Li^7 + Li^7)$	31.61	18.1
${}_{\Lambda}C^{13} \rightarrow \pi^- + Li^6 + Be^7$	15.00	4.2
${}_{\Lambda}C^{14} \rightarrow \pi^- + Li^7 + Be^7$	17.31	4.1
$({}_{\Lambda}C^{15} \rightarrow \pi^- + Li^6 + Be^9)$	22.45	8.0
$({}_{\Lambda}C^{16} \rightarrow \pi^- + Li^6 + Be^{10})$	28.04	12.5
$({}_{\Lambda}C^{16} \rightarrow \pi^- + Li^7 + Be^9)$	28.48	13.0
${}_{\Lambda}N^{14} \rightarrow \pi^- + Be^7 + Be^7$	18.67	7.0
$({}_{\Lambda}N^{16} \rightarrow \pi^- + Li^6 + B^{10})$	18.82	3.3
$({}_{\Lambda}N^{16} \rightarrow \pi^- + Be^7 + Be^9)$	17.84	2.3
$({}_{\Lambda}O^{16} \rightarrow \pi^- + Li^6 + C^{10})$	17.80	2.3 β^+ expected

The species in parenthesis have not been uniquely identified. In calculating Q, B_Λ has been inferred from the trend of the B_Λ versus A curve.

Fortunately the energy carried by the π^- in the majority of the decays shown in these tables, tends to be on the low side and does not cause too much confusion with the $(\pi^- - r)$ decays of hypernuclei with $A \leq 16$, tending instead to simulate the decay of heavier ones.

If the hyperfragments are produced under conditions where the hypothesis of production in C, N, O is valid, then quite often only the conservation of charge and baryons need be invoked in order to rule out various competing interpretations from the decay, although at other times a more detailed analysis is necessary. Without such information at production, the problem of identification is very difficult indeed.

It should also be remarked that the presence of excited states in the recoil may contribute to the misidentification of events and thereby introduce systematic errors into the measured value of B_Λ.

As mentioned earlier, the non-mesic decay modes are not usually easy to identify. In some cases however, additional information regarding the decay tracks can be of considerable help in the analysis. Such an example is shown in Fig. 6 which is interpreted as the decay

$$ {}_\Lambda Be^9 \rightarrow Li^8 + H^1 $$

in which the "hammer track" identifies the recoil as Li^8, B^8 being ruled out by considering the maximum Z possible at production. The proton appears to scatter inelastically and it is not possible to obtain a good binding energy from the event.

IV. DIRECT MASS AND CHARGE DETERMINATION

As an aid to analysis, one can also perform profile measurements to determine the charge of tracks of interest (usually that of the hyperfragment). In addition it is sometimes possible to obtain the mass by making gap-length measurements. This is of particular importance for the non-mesic decay mode of ${}_\Lambda H^{3,4}$. These events consist

of the hyperfragment decaying into only one charged particle and may be confused with Σ^- capture or Σ^+ decay via the proton mode. However, for sufficiently long connecting tracks, it is possible to distinguish a factor of ~ 3 in mass and thereby separate the non-mesic ${}_{\Lambda}H^{3,4}$ from the background. Such an analysis is under way in our laboratory[13]. In doing this we require flat tracks with $\gtrsim 1$ mm range and use the parameter η described by Ammar et al.[18].

Figure 7 shows a photomicrograph of an event which has been analysed in this manner. Mass measurement on the connecting track favours the interpretation that it is due to a particle of greater than baryonic mass. As seen from Table 4, the observed range of 4.2 mm for the secondary excludes the possibility that it comes from either of the two-body modes ${}_{\Lambda}H^4 \rightarrow H^3 + n$ or ${}_{\Lambda}H^3 \rightarrow H^2 + n$ which require a unique range of 3.5 mm and 7 mm, respectively. Mass determination

Table 4

Non-mesic decay modes of ${}_{\Lambda}H^3$ and ${}_{\Lambda}H^4$

${}_{\Lambda}H^3$	${}_{\Lambda}H^4$
$H^2 + n$ $R_d = 7$ mm	$H^3 + n$ $R_t = 3.5$ mm
$H^1 + 2n$	$H^2 + 2n$
---	$H^1 + 3n$

on the secondary also favours its interpretation as a particle of greater than baryonic mass. The event can therefore most likely be interpreted as

$$ {}_{\Lambda}H^4 \rightarrow H^2 + 2n \ . $$

It should be emphasized, however, that events analysed in this manner are subject to far more uncertainty than those identified entirely by kinematic considerations, and as a result their significance rests more on a statistical basis than on an individual one.

Although the yield is low, it is hoped that by the accumulation of such events, normalized to the appropriate number of π^- decays of ${}_{\Lambda}H^{3,4}$, one can determine a precise value of the non-mesic to π^--mesic ratio for these hyperfragments directly.

* * *

REFERENCES

1) F.C. Gilbert, C.E. Violet and R.S. White, Phys.Rev. 103, 248 (1956).

2) B.P. Bannik, U.G. Guliamov, D.K. Kopylova, A.A. Nomofilov, M.I. Podgoreetskii, B.G. Rakhimbaev and M. Usmanova, Sov.Phys. JETP 7, 198 (1958).

3) P.H. Fowler, Phil.Mag. 3, 1460 (1958).

4) P.E. Schlein and W.E. Slater, Nuovo Cimento 21, 213 (1961).

5) R.G. Ammar, L. Choy, W. Dunn, M. Holland, J.H. Roberts, E.N. Shipley, N. Crayton, D.H. Davis, R. Levi Setti, M. Raymund, O. Skjeggestad and G. Tomasini: "Binding energies of hypernuclei with mass number A > 5". Submitted to Nuovo Cimento.

6) D.J. Prowse, Physics Letters 1, 178 (1962).

7) B. Blowmik, Physics Letters 2, 220 (1962).

8) J. Schneps, W.F. Fry and M. Swami, Phys.Rev. 106, 1062 (1957).

9) J. Sacton, Kiev Conference (1959), reported by E.H.S. Burhop: UCRL-9354.

10) V. Gorge, W. Koch, W. Lindt, M. Nikolić, S. Subotic-Nicolić and H. Winzeler, Nucl.Phys. 21, 599 (1961).

11) O.E. Overseth, Bull.Am.Phys.Soc. 6, 39 (1961).

5683/NP/kw

12) D. Abeledo, L. Choy, R.G. Ammar, N. Crayton, R. Levi Setti, M. Raymund and O. Skjeggestad, Nuovo Cimento 22, 1171 (1961).

13) M.W. Holland, R.G. Ammar, A. Behkami and J.H. Roberts, Bull.Am. Phys.Soc. 8, 349 (1963).

14) M.W. Holland: thesis, in course of preparation.

15) W.E. Slater, Suppl. Nuovo Cimento 10, 1 (1958).

16) R. Ammar, R. Levi Setti, W.E. Slater, S. Limentani, P.E. Schlein and P.H. Steinberg, Nuovo Cimento 15, 181 (1960).

17) N. Crayton, R. Levi Setti, M. Raymund, O. Skjeggestad, D. Abeledo, R.G. Ammar, J.H. Roberts and E.N. Shipley, Rev.Mod.Phys. 34, 186 (1962).

18) R.G. Ammar, N. Crayton, K.P. Jain, R. Levi Setti, J.E. Mott, P.E. Schlein, O. Skjeggestad and P.K. Srivastava, Phys.Rev. 120, 1914 (1960).

* * *

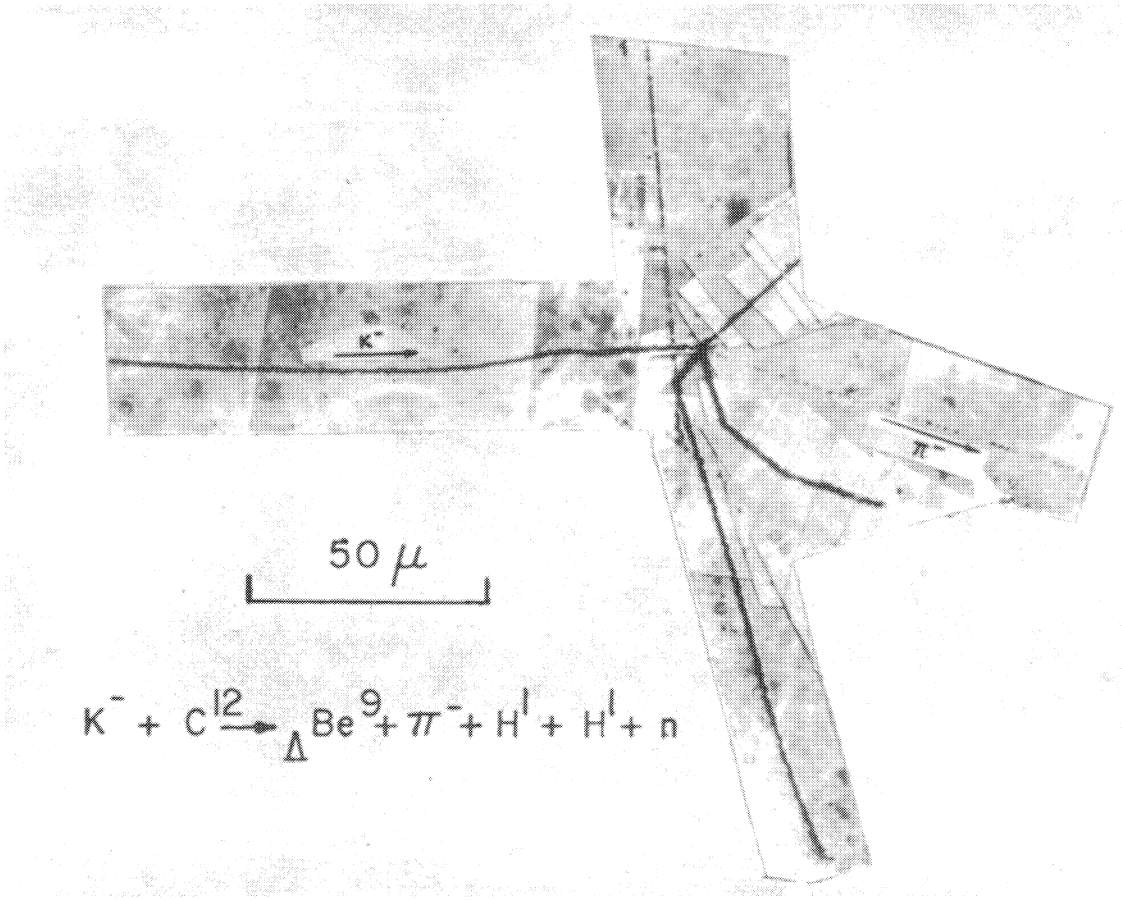

Fig. 1. - Photomicrograph of event interpreted as $K^- + C^{12} \rightarrow {}_{\Lambda}Be^9 + H^1 + H^1 + n + \pi^-$.

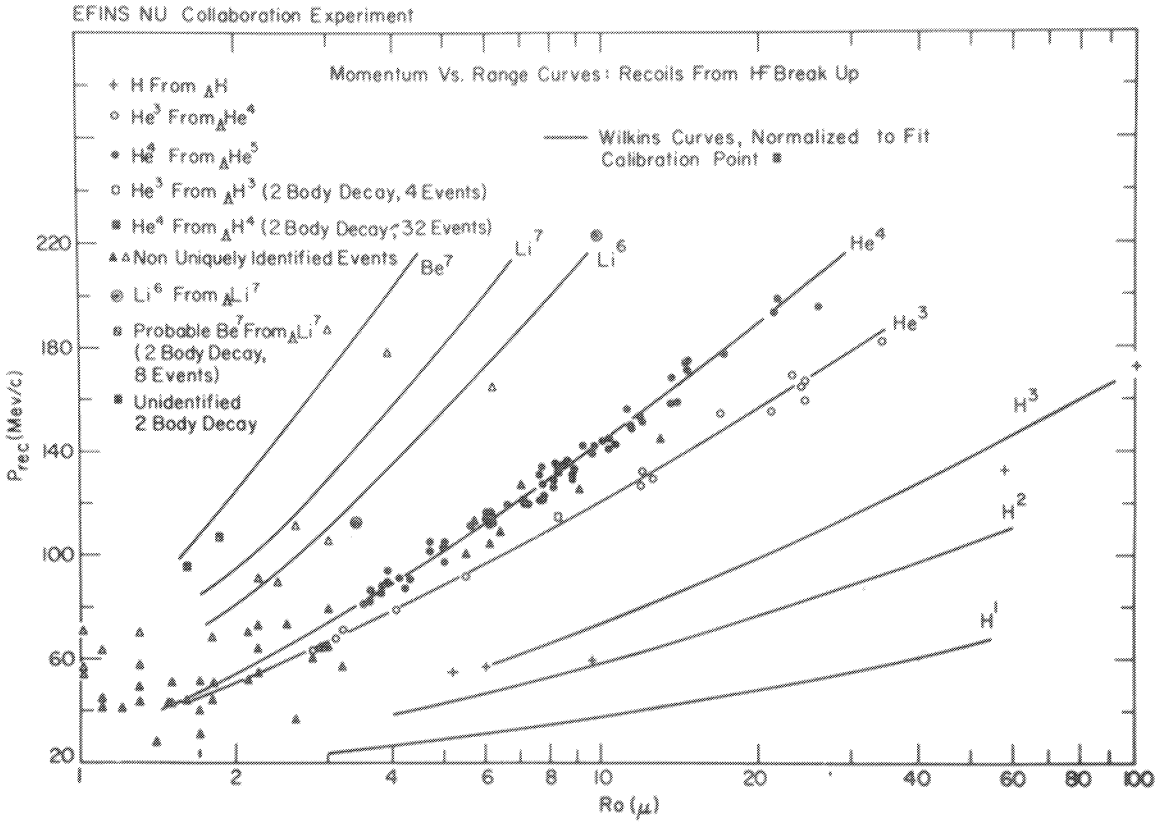

Fig. 2. - Range vs. momentum curves for recoils from hyperfragment decays.

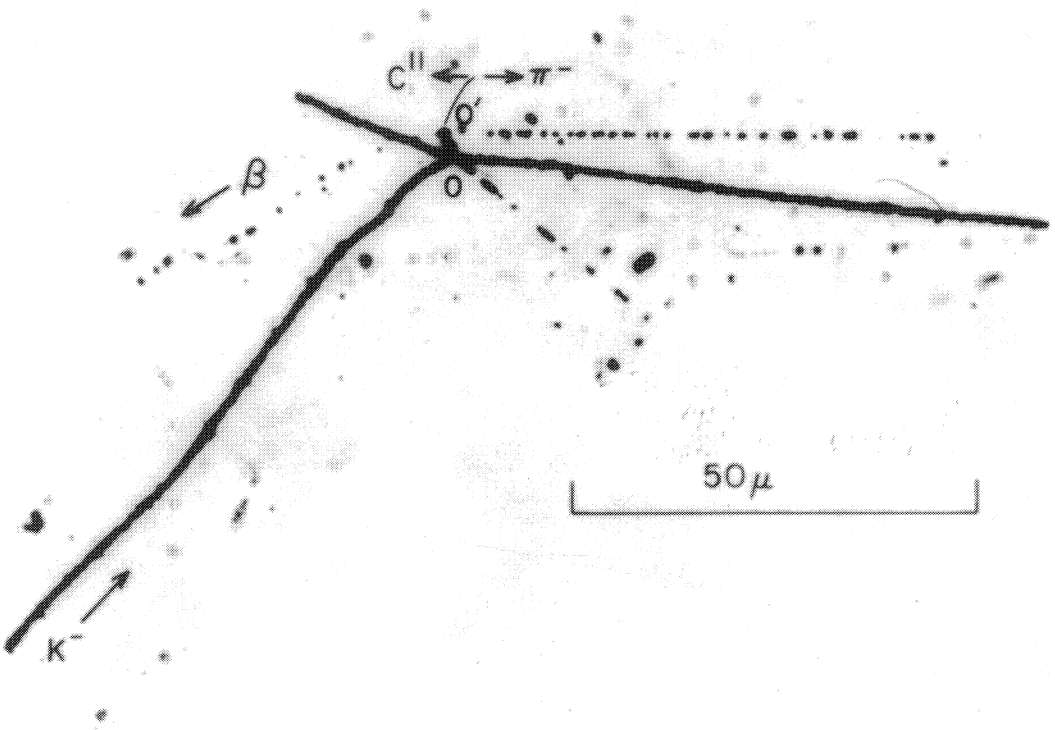

Fig. 3. - Photomicrograph of event interpreted as ${}_{\Lambda}B^{11} \to \pi^{-} + C^{11}$.

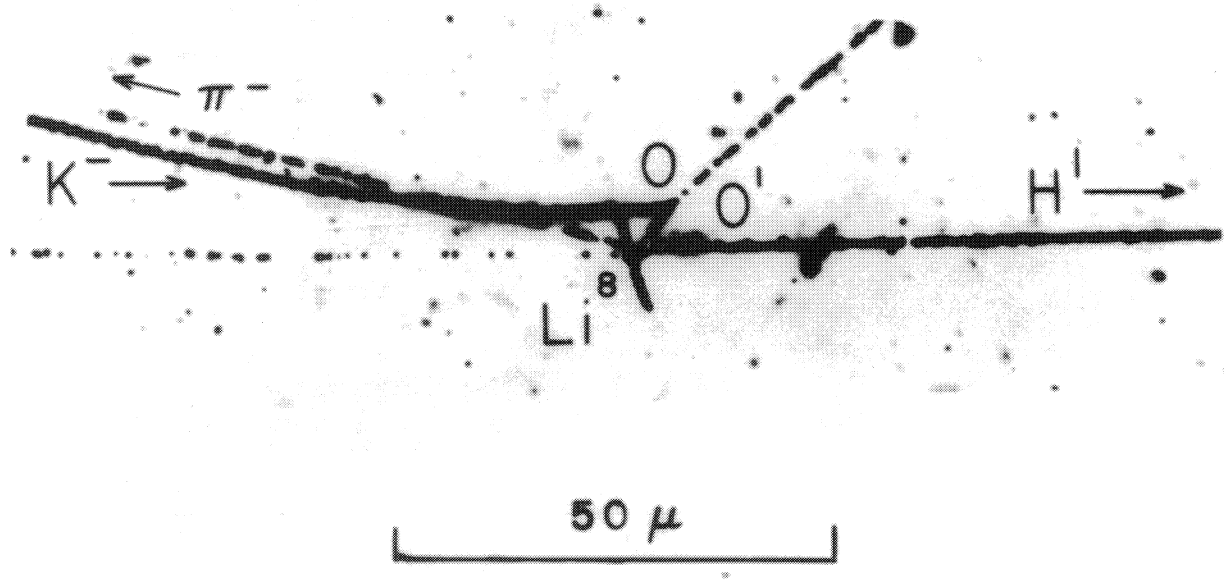

Fig. 4. - Photomicrograph of event interpreted as ${}_{\Lambda}Li^{9} \to \pi^{-} + H^{1} + Li^{8}$.

$$ {}_{\Lambda}Z^{A} \rightarrow (Z+1)^{A} + \pi^{-} $$
$$ 6 \leq A \leq 16 $$

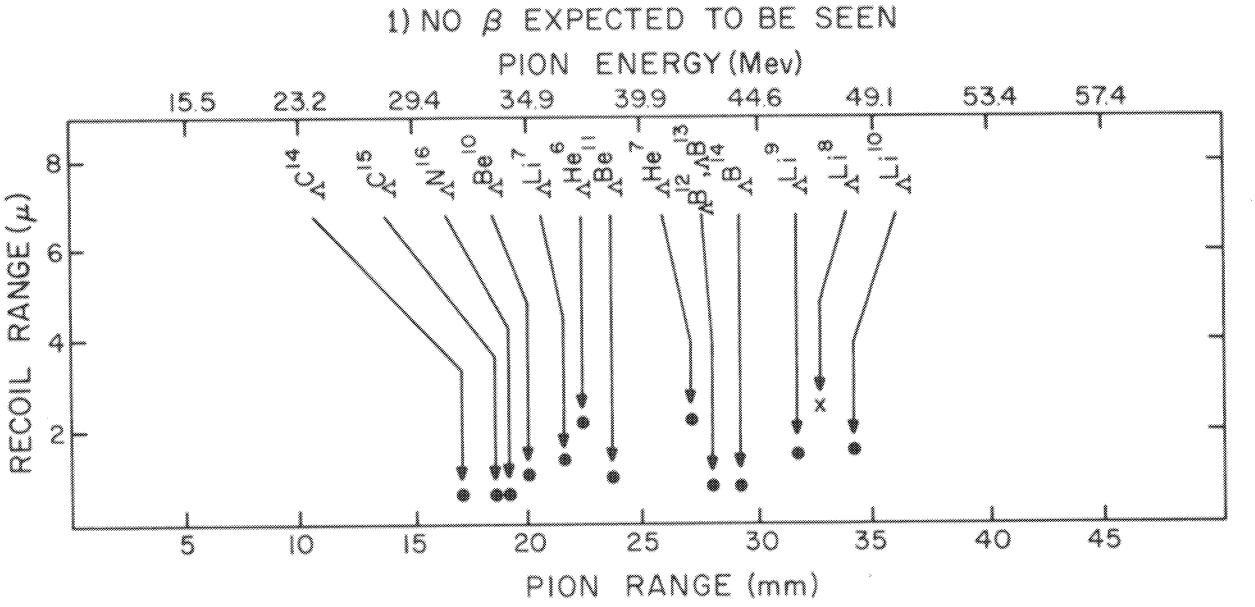

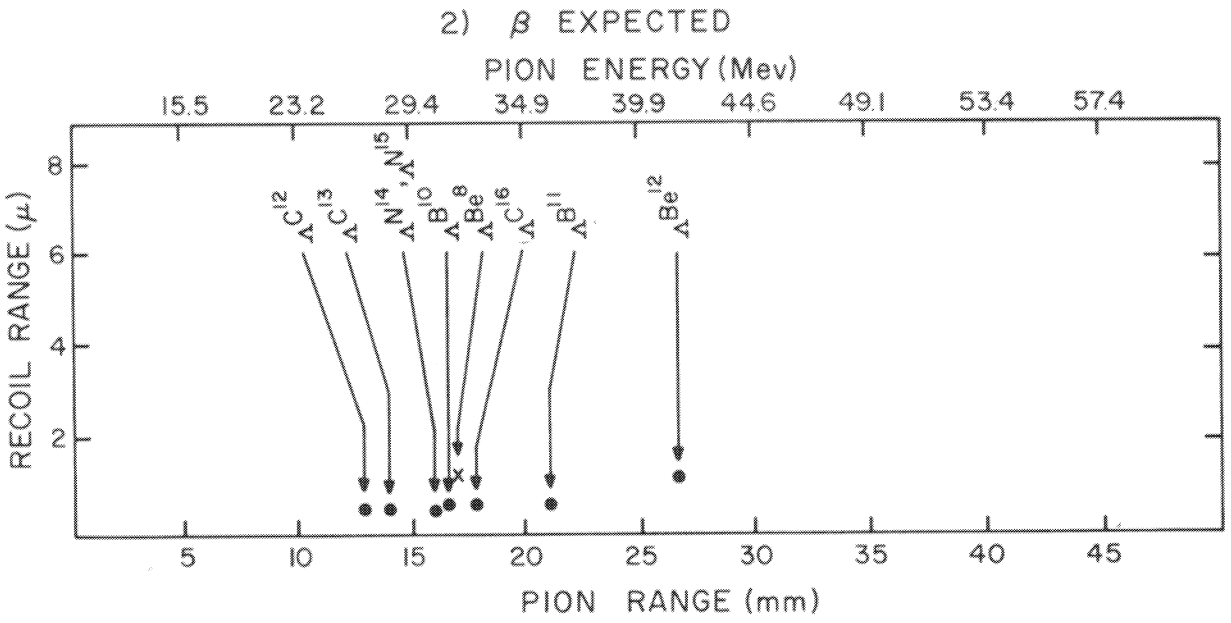

Fig. 5. - (π^{-} - r) Configurations displayed in two groups according as the lifetime for β decay of the recoil is long or short compared with the sensitive time of the emulsion. Several species shown have not been actually observed and for these the B_{Λ} used in calculating the energy release has been estimated from the trend of the B_{Λ} vs. A curve. Events denoted by x have recoils which decay into heavy particles.

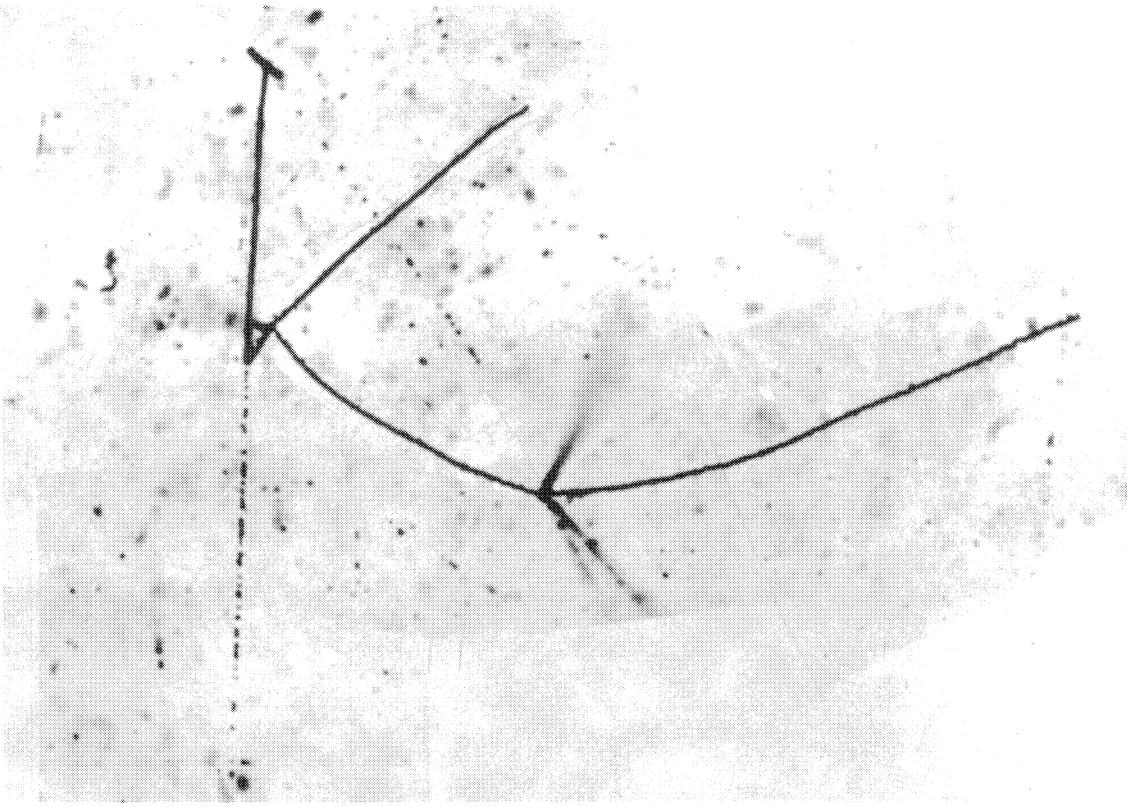

Fig. 6. - Photomicrograph of event interpreted as ${}_{\Lambda}Be^{9} \rightarrow Li^{8} + H^{1}$.

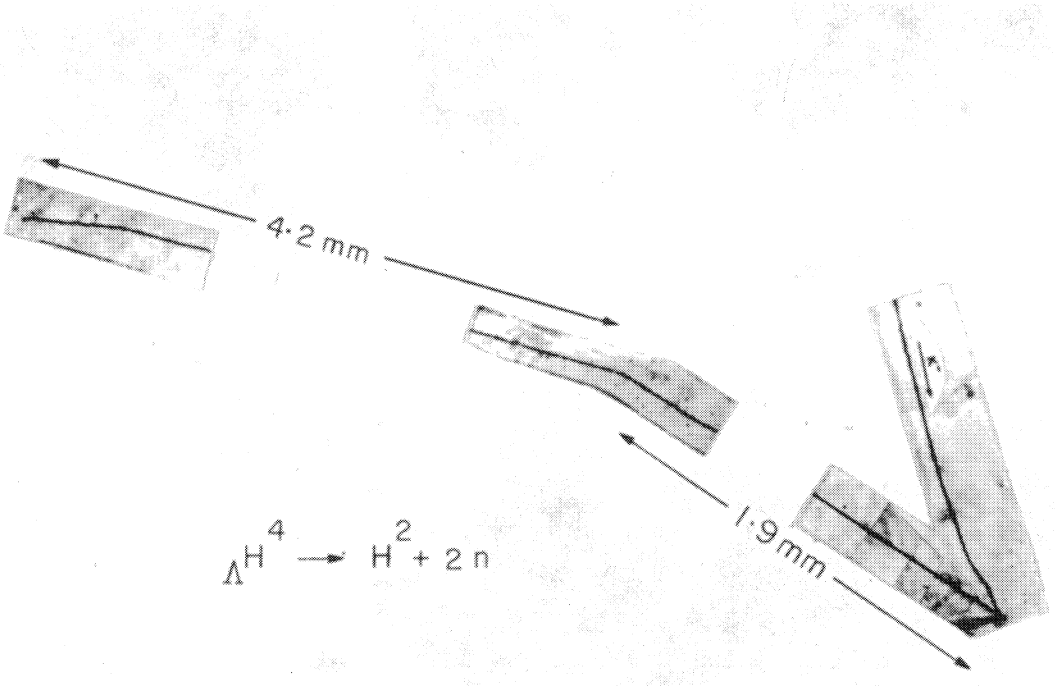

Fig. 7. - Photomicrograph of event interpreted as ${}_{\Lambda}H^{4} \rightarrow H^{2} + 2n$.